

Impact of Boron Nitride Additive on the Phase Formation and Transport Properties of Bi(Pb)-2223 Superconductor

A. S. Kuzanyan^{a,*}, N. G. Margiani^b, G. A. Mumladze^b, I. G. Kvartskhava^b,
G. R. Badalyan^a, and V. V. Zhghamadze^b

^aInstitute for Physical Research, NAS of Armenia, Ashtarak, Armenia

^bInstitute of Cybernetics. Vladimir Chavchanidze Georgian Technical University, Tbilisi, Georgia

*e-mail: akuzanyan@yahoo.com

Received January 29, 2020; revised February 25, 2020; accepted March 5, 2020

Abstract—Doping of a high-temperature Bi(Pb)-2223 superconductor with various additives, which can act as pinning centers and / or accelerate the formation of a superconducting phase, is an effective tool for obtaining Bi(Pb)-2223 samples with improved characteristics. In this paper, we studied the effect of the addition of hexagonal boron nitride (*h*-BN) on the phase formation and critical transport current density of ceramic samples Bi(Pb)-2223. Samples with a nominal composition of $\text{Bi}_{1.7}\text{Pb}_{0.3}\text{Sr}_2\text{Ca}_2\text{Cu}_3\text{O}_y$ [BN]_{*x*}, *x* = 0–0.25 were prepared by the solid-phase reaction method. Two different doping methods were used: the introduction of hand-ground BN powder at the initial stage of synthesis and the addition of BN powder subjected to high-energy grinding in a ball mill before pelletizing. The phase composition of the obtained samples was studied by X-ray diffraction. The microstructure and elemental composition of the samples were studied using a scanning electron microscope with an X-ray microanalyzer. The resistivity and critical current density were measured using the standard four-probe method. The results show that boron nitride is a suitable additive to increase the rate of formation and critical transport current density Bi(Pb)-2223.

Keywords: Bi(Pb)-2223 phase, doping, high energy ball milling, phase formation, critical current density

DOI: 10.3103/S1068337220030081

1. INTRODUCTION

Undoubtedly, the discovery of high-temperature superconductivity (HTSC) at $T_c = 38$ K in LSCO cuprates was one of the most significant achievements of 20th-century science [1]. Thanks to efforts of different research groups, the critical temperature of a new class of superconductors increased rapidly. Superconductivity was found in YBCO ($T_c = 93$ K) [2], Tl-2201 ($T_c = 95$ K) and Tl-2223 ($T_c = 125$ K) [3, 4], Bi-2212 ($T_c = 95$ K) and Bi-2223 ($T_c = 110$ K) [5, 6]. Among the first researchers in this new direction were also representatives of the Institute for Physical Research of the NAS of Armenia and the Institute of Cybernetics of Technical University of Georgia. In particular, the effect of more than fifteen impurities on the superconducting properties of the Bi-2223 phase and the formation of unstable magnetic anomalies in Bi-containing cuprates were studied in detail [7–16]. Among the high-temperature superconducting materials, the compound Bi(Pb)-2223 is one of the most promising for applications in science and technology. The synthesis of single-phase Bi-2223 is a difficult problem since the kinetics of phase formation is very slow. To obtain a material with a high volume fraction of the Bi(Pb)-2223 phase, heat treatment is required for a duration of 150–200 h [17, 18]. In addition, the extremely narrow temperature stability range of Bi(Pb)-2223 leads to the formation of secondary phases (Bi-2201, Bi-2212, Ca_2PbO_4 , etc.) [19, 20]. Many applications of cuprate superconductors are due to an increase in their manufacturability and resistance to external influences. This task is still relevant today. Modification of the structural and superconducting properties of the Bi(Pb)-2223 phase using various micron and nanoscale dopants, which can act as effective pinning centers and/or accelerate the formation of the HTSC phase, is an effective tool for the synthesis of Bi(Pb)-2223 samples with improved characteristics [21–23]. The correlation between synthesis conditions, structural, microstructural and superconducting properties is not well understood. Based on the foregoing, obtaining samples with a maximum Bi(Pb)-2223 phase content is still considered a difficult task requiring further research [20, 22, 24, 25].

Our previous results show that the addition of boron nitride (BN) promotes the formation of the Bi-2223 phase and leads to an increase in the critical transport current density (J_c) as compared to the undoped (control) sample [26]. In this article, we report on the further study of two sets of ceramic samples Bi(Pb)-2223, doped with different amounts of hand-ground boron nitride powder and subjected to high-energy grinding in a planetary mill.

2. THE EXPERIMENTAL TECHNIQUE

Samples of the nominal composition $\text{Bi}_{1.7}\text{Pb}_{0.3}\text{Ca}_2\text{Sr}_2\text{Cu}_3\text{O}_y(\text{BN})_x$ ($x = 0.10, 0.15, 0.20, \text{ and } 0.25$) undoped and doped with BN were obtained by solid-phase synthesis from Bi_2O_3 , PbO , SrCO_3 , CaCO_3 , CuO , and hexagonal BN powders (purity 98%). Two different doping methods were used: the introduction of manual grinding BN additive at the initial stage of synthesis (samples of series A), the addition of powdered BN powder in a ball mill before tableting (samples of series B). The starting powders were thoroughly ground, mixed, and calcined at $800\text{--}820^\circ\text{C}$ for 12 hours; the synthesis was carried out at 850°C for 40 hours on alundum boats with intermediate grinding. Additive BN was subjected to high-energy grinding in a ball planetary mill (Fritsch Pulverisette 7 Premium Line) for 10 hours at a speed of 350 rpm. Eighty ZrO_2 balls with a diameter of 5 mm were used as the grinding medium. The mass ratio of the balls and powder was approximately 15 : 1. After grinding, the corresponding amounts of BN were mixed with the Bi(Pb)-2223 precursor. Then, two series of Bi(Pb)-2223 powders were pressed into pellets with a diameter of 10 mm at a hydrostatic pressure of 500 MPa. The pellets were annealed at 850°C for 30 h in air, followed by cooling of the furnace to room temperature. As a result of synthesis, 9 samples were obtained: a general control sample without BN impurity (marking R), four samples of series A doped with hand-boron boron nitride (markings A1–A4) and four samples of series B doped with boron nitride subjected to high-energy grinding in ball mill (marking B1–B4) with the content of the additive (BN) x at $x = 0.10, 0.15, 0.20$ and 0.25 , respectively.

The obtained samples were investigated by the following methods. The phase composition was studied by powder diffractometry using $\text{CuK}\alpha$ radiation on a Dron-3M diffractometer (XRD). The microstructure and elemental composition were studied using a VEGA TS5130MM scanning electron microscope (SEM) and the INCA Energy 300 (EDX) energy dispersive X-ray microanalysis system. The resistivity $\rho(T)$ in the temperature range $300\text{--}77$ K and the critical density of the transport current J_c at 77 K were measured by the standard four-probe method on rod-shaped samples with sizes of $\sim 10 \times 0.5 \times 0.5$ mm³.

3. RESULTS AND DISCUSSION

3.1. X-Ray Analysis (XRD) and Transport Measurements

Figure 1 shows the diffraction patterns of two sets of ceramic Bi(Pb)-2223 samples doped with various amounts of boron nitride. In the undoped sample, the main ones are Bi(Pb)-2223 and Bi(Pb)-2212 phases. Both doping methods lead to an increase in the Bi(Pb)-2223 phase peaks with a simultaneous decrease in the intensities of the Bi(Pb)-2212 peaks in the range of the dopant content $x = 0.10\text{--}0.20$. At the same time, the diffraction patterns of doped samples of series A show the appearance of a weak peak of the impurity Bi-2201 phase, the intensity of which increases with increasing BN content. In the same series, at $x \geq 0.15$, a low-intensity peak of the Ca_2PbO_4 impurity phase is seen.

The content of Bi(Pb)-2223 phase in the synthesized samples was estimated using the formula [22]:

$$V(2223)\% = \frac{\sum H}{\sum H + \sum L + \sum(\text{others})} \times 100,$$

where $\sum H$, $\sum L$, and $\sum(\text{others})$ represent the sum of the intensities of the observed peaks of the high-temperature 2223 phase, low-temperature 2212, and other impurity phases, respectively. Figure 2 shows the dependence of the volume fraction of the Bi(Pb)-2223 phase on the concentration of BN.

The content of Bi(Pb)-2223 phase in the standard sample is 60%. Doping with boron nitride at $x = 0.20$ leads to an increase in the proportion of the Bi(Pb)-2223 phase to 76 and 82% in series A and B, respectively. With a further increase in the additive concentration, a decrease in the volume fraction of Bi(Pb)-2223 is observed in both series. Figure 3 shows the temperature dependences of the resistivity of samples of series A and B. All samples are characterized by a metallic type of conductivity above the onset of the superconducting transition $T_c(\text{on})$. The temperature of zero resistance, $T_c(\text{off})$, of the standard sample R is 104.5 K. For samples of series A in the interval of the dopant content $x = 0.10\text{--}0.20$, the value of $T_c(\text{off})$ remains prac-

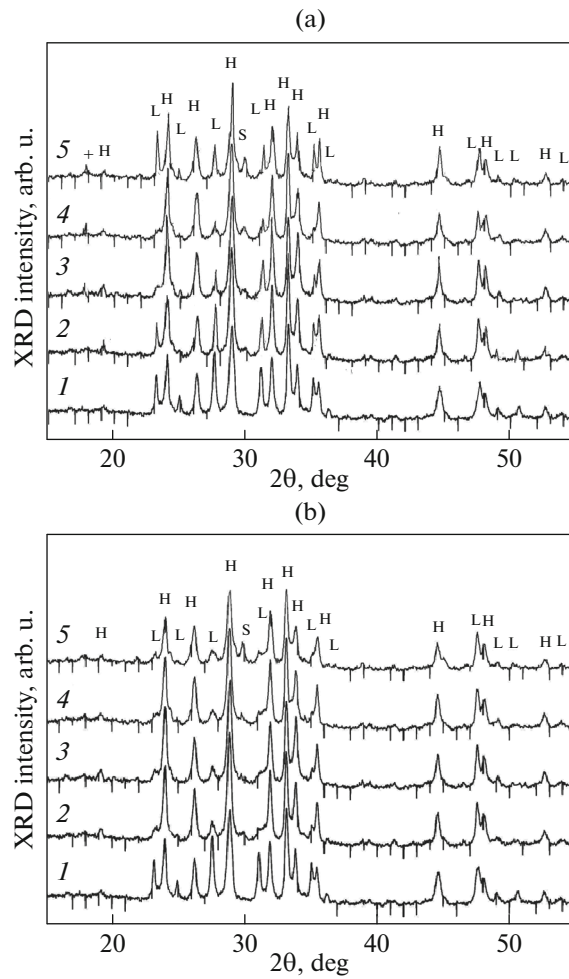


Fig. 1. X-ray diffraction patterns of $\text{Bi}_{1.7}\text{Pb}_{0.3}\text{Ca}_2\text{Sr}_2\text{Cu}_3\text{O}_y(\text{BN})_x$ series A—(a) and B—(b). 1— $x = 0$, 2— $x = 0.10$, 3— $x = 0.15$, 4— $x = 0.20$ and 5— $x = 0.25$. H: Bi(Pb)-2223, L: Bi(Pb)-2212, S: Bi(Pb)-2201, +: Ca_2PbO_4 .

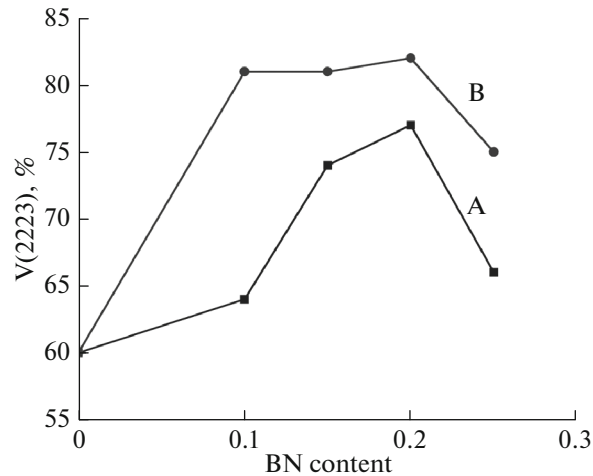


Fig. 2. Volume fraction of Bi(Pb)-2223 phase depending on the BN content in $\text{Bi}_{1.7}\text{Pb}_{0.3}\text{Ca}_2\text{Sr}_2\text{Cu}_3\text{O}_y(\text{BN})_x$ samples of series A and B.

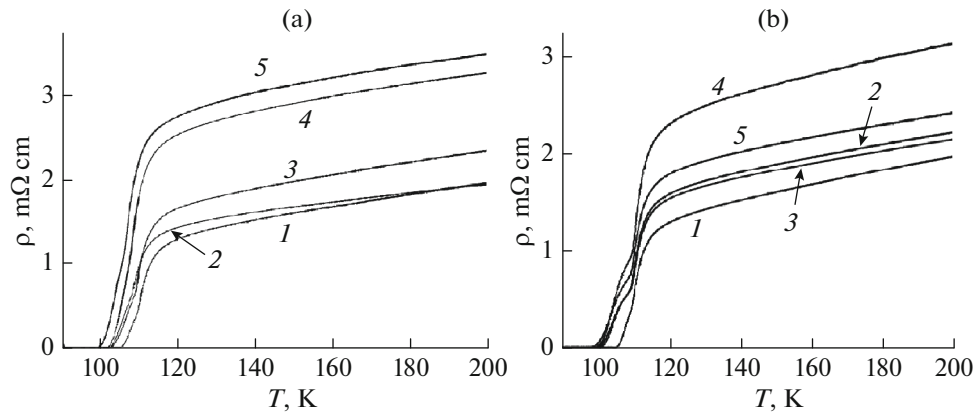


Fig. 3. Temperature dependence of the resistivity of $\text{Bi}_{1.7}\text{Pb}_{0.3}\text{Ca}_2\text{Sr}_2\text{Cu}_3\text{O}_y(\text{BN})_x$ samples of series A—(a) and B—(b). 1— $x = 0$, 2— $x = 0.10$, 3— $x = 0.15$, 4— $x = 0.20$ and 5— $x = 0.25$.

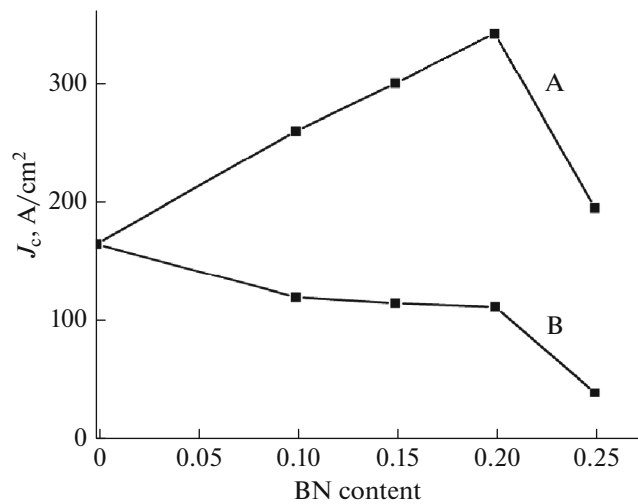


Fig. 4. Dependence of the critical current density on the BN content in $\text{Bi}_{1.7}\text{Pb}_{0.3}\text{Ca}_2\text{Sr}_2\text{Cu}_3\text{O}_y(\text{BN})_x$ samples of series A and B.

tically unchanged and amounts to 102 K. A further increase in the concentration of BN to $x = 0.25$ leads to a decrease in the temperature of zero resistance to 99 K.

Unlike series A, doped samples of series B are characterized by a pronounced two-stage superconducting transition, which indicates a deterioration in the quality of intergranular contacts as a result of the addition of high-energy grinding dopant. The value of $T_c(\text{off})$ of series B samples decreases monotonically with an increase in the concentration of BN additive and amounts to 97.5 K at $x = 0.25$.

The dependences of the critical current density, J_c , on the BN content in the samples under study are given in Fig. 4. The addition of BN to the $\text{Bi}_{1.7}\text{Pb}_{0.3}\text{Ca}_2\text{Sr}_2\text{Cu}_3\text{O}_y$ precursor at the initial stage of the synthesis leads to a sharp increase in J_c . The critical current density for an undoped sample is 165 A/cm^2 . J_c increases with increasing BN content in series A samples and at $x = 0.20$ reaches 342 A/cm^2 . A further increase in the dopant concentration to $x = 0.25$ leads to a decrease in the critical current density as a result of an increase in the content of impurities 2212 and 2201 phases observed in the diffraction pattern of sample A4.

Doping Bi(Pb)-2223 before pelletizing samples of series B leads to a decrease in J_c in the entire studied range of BN content, especially sharp at $x = 0.25$. This result is consistent with the appearance of a pronounced two-stage superconducting transition in samples of this series (Fig. 3). Figure 5 shows the dependence of the density of the synthesized samples on the content of the BN additive. In series A, doping leads

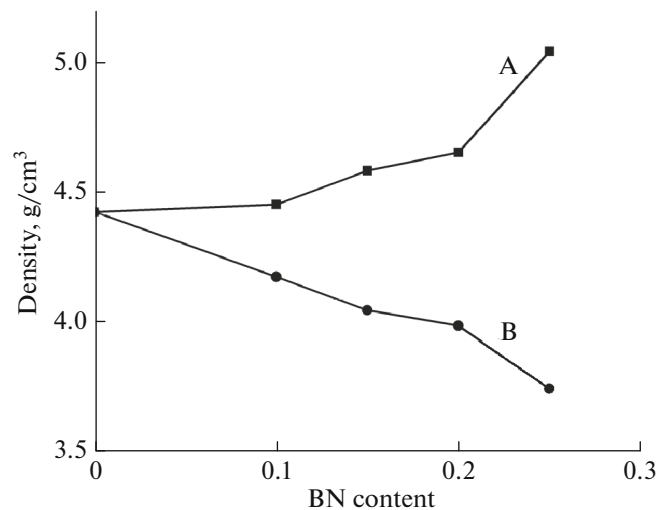


Fig. 5. Dependence of the density of $\text{Bi}_{1.7}\text{Pb}_{0.3}\text{Ca}_2\text{Sr}_2\text{Cu}_3\text{O}_y(\text{BN})_x$ samples of series A and B on the content of BN.

to a monotonic increase in the density of samples (from 4.42 g/cm^3 for sample R to 5.04 g/cm^3 for sample A4 with a dopant content $x = 0.25$), which contributes to an increase in the critical current density in this series.

The introduction of the additive before pelletizing, on the contrary, leads to a sharp decrease in density, which for sample B4 is 3.74 g/cm^3 , i.e. the density at $x = 0.25$ decreases by 26% compared with the undoped sample. An increase in the porosity of series B samples with increasing dopant concentration favors J_c degradation.

3.2. Scanning Electron Microscopy (SEM)

The density of the critical transport current depends both on the density of the superconducting material and on the degree of texturing [27]. The microstructure of the samples was studied using an electron microscope at an accelerating voltage of 20 kV and an electron probe current of 10–100 pA in a vacuum of 5×10^{-5} Torr. Samples were mounted inside the vacuum chamber of the microscope on an aluminum holder. No further purification or metallization of the samples was carried out. Images of the surface of the samples in secondary electrons with an increase of $1000\times \dots 30000\times$ were obtained.

Figure 6 shows micrographs of the surface of BN powder subjected to high-energy grinding in a ball mill with a magnification of $2000\times$, a control sample, and samples of two series A3, A4 and B3, B4 with a magnification of $3000\times$.

As can be seen from Fig. 6, as a result of high-energy grinding, micron and submicron agglomerates are formed in boron nitride powder. In the control sample R, both acicular and lamellar crystallites characteristic of Bi-2212 and Bi-2223 phases, respectively, are observed [28]. Doped Bi(Pb)-2223 samples consist mainly of lamellar crystallites with sizes of 5–15 μm . Small inclusions of spherical granules with a diameter of $\sim 0.2\text{--}1 \mu\text{m}$ are noticeable. There is a noticeable difference between the samples of series A and samples of series B. With approximately the same granule shape, the samples of series A have a much lower grain misorientation compared to samples of series B and the crystallites have a predominant orientation parallel to the flat surface of the tablets. With an increase in the amount of BN additive to $x = 0.25$, a simultaneous increase in the average disorientation of crystallites and the degree of porosity is clearly observed in sample B4.

3.3. Energy Dispersive X-ray Microanalysis (EDX)

Energy dispersive X-ray microanalysis of the samples was carried out on surface areas with an area of about $40 \times 40 \mu\text{m}^2$ at an accelerating voltage of 20 kV. The statistical error in determining the content of Bi, Pb, Sr, Ca, Cu, and O elements in the samples was 0.18, 0.19, 0.24, 0.26, 0.39, and 1.54 at %, respectively. To determine the homogeneity of the composition, some samples were studied at various surface sites. The research results are presented in the Table 1, which shows the number of the sample and the

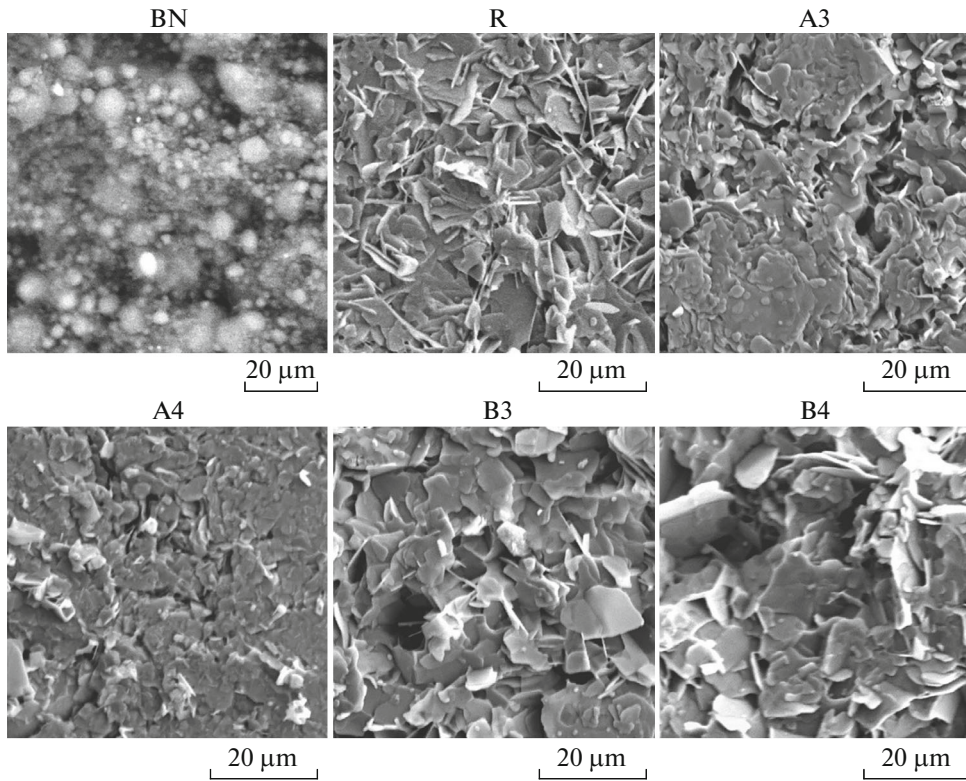


Fig. 6. Microphotographs of high-energy milled BN powder, control sample (R), and samples of the two series A3, A4 and B3, B4.

Table 1. Results of X-ray microanalysis of samples

Number of samples	Atomic percent						Chemical formula
	Bi	Pb	Sr	Ca	Cu	O	
R	10.22	1.12	10.62	9.59	15.89	52.56	$\text{Bi}_{1.80}\text{Pb}_{0.20}\text{Sr}_{1.87}\text{Ca}_{1.69}\text{Cu}_{2.80}\text{O}_{9.27}$
	10.12	0.97	10.21	10.73	15.44	52.53	$\text{Bi}_{1.83}\text{Pb}_{0.17}\text{Sr}_{1.84}\text{Ca}_{1.94}\text{Cu}_{2.78}\text{O}_{9.47}$
A1	9.49	1.46	9.89	10.12	16.66	52.37	$\text{Bi}_{1.73}\text{Pb}_{0.27}\text{Sr}_{1.81}\text{Ca}_{1.85}\text{Cu}_{3.04}\text{O}_{9.57}$
	9.75	1.42	9.89	10.26	16.25	52.44	$\text{Bi}_{1.75}\text{Pb}_{0.25}\text{Sr}_{1.77}\text{Ca}_{1.84}\text{Cu}_{2.91}\text{O}_{9.39}$
A2	9.91	1.26	9.44	10.66	16.26	52.48	$\text{Bi}_{1.77}\text{Pb}_{0.23}\text{Sr}_{1.69}\text{Ca}_{1.91}\text{Cu}_{2.91}\text{O}_{9.40}$
	9.60	1.37	9.56	10.87	16.19	52.40	$\text{Bi}_{1.75}\text{Pb}_{0.25}\text{Sr}_{1.74}\text{Ca}_{1.98}\text{Cu}_{2.95}\text{O}_{9.55}$
A3	9.38	1.31	9.18	11.00	16.79	52.34	$\text{Bi}_{1.75}\text{Pb}_{0.25}\text{Sr}_{1.72}\text{Ca}_{2.06}\text{Cu}_{3.14}\text{O}_{9.79}$
A4	10.09	0.78	11.11	10.99	14.51	52.52	$\text{Bi}_{1.86}\text{Pb}_{0.14}\text{Sr}_{2.04}\text{Ca}_{2.03}\text{Cu}_{2.67}\text{O}_{9.66}$
B1	9.48	1.60	10.08	10.04	16.43	52.37	$\text{Bi}_{1.71}\text{Pb}_{0.29}\text{Sr}_{1.82}\text{Ca}_{1.81}\text{Cu}_{2.97}\text{O}_{9.45}$
B2	9.32	1.43	9.87	10.74	16.30	52.33	$\text{Bi}_{1.73}\text{Pb}_{0.27}\text{Sr}_{1.84}\text{Ca}_{2.00}\text{Cu}_{3.03}\text{O}_{9.74}$
B3	9.32	1.54	9.15	10.92	16.74	52.33	$\text{Bi}_{1.72}\text{Pb}_{0.28}\text{Sr}_{1.69}\text{Ca}_{2.01}\text{Cu}_{3.08}\text{O}_{9.64}$
	9.84	1.31	9.29	10.72	16.38	52.46	$\text{Bi}_{1.77}\text{Pb}_{0.23}\text{Sr}_{1.67}\text{Ca}_{1.92}\text{Cu}_{2.94}\text{O}_{9.41}$
B4	9.24	1.27	9.88	10.14	17.17	52.31	$\text{Bi}_{1.76}\text{Pb}_{0.24}\text{Sr}_{1.88}\text{Ca}_{1.93}\text{Cu}_{3.27}\text{O}_{9.95}$
	9.07	1.21	9.95	10.18	17.32	52.27	$\text{Bi}_{1.76}\text{Pb}_{0.24}\text{Sr}_{1.94}\text{Ca}_{1.98}\text{Cu}_{3.37}\text{O}_{10.17}$
	8.97	1.45	9.77	9.87	17.71	52.24	$\text{Bi}_{1.72}\text{Pb}_{0.28}\text{Sr}_{1.88}\text{Ca}_{1.89}\text{Cu}_{3.40}\text{O}_{10.03}$

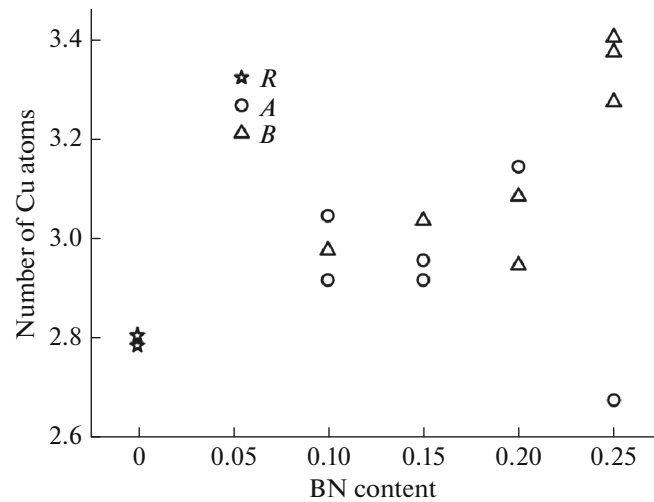


Fig. 7. The number of copper atoms in the chemical formula of samples *R*, as well as *A* and *B* with different amounts of BN additives.

content of elements in atomic percent. The table also shows the chemical formulas based on the assumption that the total number of bismuth and lead atoms in the chemical formula found in the sample corresponds to the number 2.

As can be seen from the Table, the composition of the control sample *R* is quite uniform. In two analyzes, the oxygen concentration differs by thousandths of atomic percent, bismuth by 0.1 at %, while the statistical error for bismuth is almost two times greater. The differences in the concentrations of the remaining elements with the exception of calcium also do not exceed the statistical error. It can be argued that the control sample has a uniform composition. A similar pattern is observed for samples *A1*, *A2*, and *B3*, in which the composition was analyzed in two regions and *B4* in three. We conclude that the technology used makes it possible to obtain ceramic samples of both series homogeneous in composition.

We proceed to a comparison of the compositions of various samples. From the data of the table on oxygen concentration it follows that the maximum content of 52.56 at % has a control *R* sample, and the minimum content of 52.24 at % sample *B4*, i.e. Sample with maximum BN additive content. However, these two digits differ slightly, and this difference is much less error. It can be assumed that the same oxygen content in the samples indicates the same valence composition of cations with variable valency.

The superconducting properties in bismuth superconductors are determined by the phase composition, and the phases differ in the number of copper layers in the unit cell. In this regard, it is interesting to compare the concentration of copper in the samples. This is conveniently done using the number of copper atoms in the calculated chemical formulas. The data for the control sample and samples of both synthesized series are shown in Fig. 7.

As can be seen from the Fig. 7, samples with an average content of BN additive ($x = 0.10, 0.15, 0.20$) have close to the stoichiometric value of 3. It can be assumed that precisely these samples should have higher superconducting properties. The Cu content in samples with a high content of BN additive ($x = 0.25$) is much lower than the stoichiometric in series *A*, and higher than the stoichiometric in series *B*. It is difficult to assume that these samples will have high superconducting properties.

4. CONCLUSION

The features of phase formation, the critical transport current density, and the microstructure of two series of ceramic samples $\text{Bi}_{1.7}\text{Pb}_{0.3}\text{Sr}_2\text{Ca}_2\text{Cu}_3\text{O}_y[\text{BN}]_x$ ($x = 0-0.25$) with the addition of hexagonal boron nitride of manual grinding and subjected to high-energy grinding in a planetary mill are studied. Additive BN accelerates the formation of the high-temperature phase in the samples of both series. The optimal doping of boron nitride with the manual grinding of the *Bi(Pb)*-2223 precursor before the start of heat treatment leads to an increase in the critical density of the transport current in series *A* samples by about 2 times compared with the control sample. However, the addition of high-energy milled dopant to *Bi(Pb)*-2223 at the final synthesis stage (before pelletizing samples of series *B*) causes a decrease in J_c , which is caused by a noticeable decrease in the density of samples and an increase in the degree of disorientation of crystallites with an increase in the level of doping.

FUNDING

This work was supported by Shota Rustaveli National Science Foundation of Georgia (SRNSF) [DI-18-479/Development of advanced bismuth-based superconducting materials via doping and high-energy ball-milling].

CONFLICT OF INTEREST

The authors declare that they have no conflict of interest.

REFERENCES

1. Bednorz, J.G. and Muller, K.A., *Z. Phys. B*, 1986, vol. 64, p. 189.
2. Wu, M.K., Ashburn, J.R., Torng, C.J., Hor, P.H., Meng, R.L., Gao, L., Huang, Z.J., Wang, Y.Q., and Chu, C. W., *Phys. Rev. Lett.*, 1987, vol. 58, p. 908.
3. Sheng, Z.Z. and Hermann, A.M., *Nature (London)*, 1988, vol. 332, p. 55.
4. Sheng, Z. and Hermann, A., *Nature*, 1988, vol. 332, p. 138.
5. Maeda, H., Tanaka, Y., Fukutomi, M., and Asano, T., *Jpn. J. Appl. Phys.*, 1988, vol. 27, p. L209.
6. Hazen, R.M., Prewitt, C.T., Angel, R.J., Ross, N.L., Finger, L.W., Hadidiacos, C.G., Veblen, D.R., Heaney, P.J., Hor, P.H., Meng, R.L., Sun, Y.Y., Wang, Y.Q., Xue, Y.Y., Huang, Z.J., Gao, L., Bechtold, J., and Chu, C.W., *Phys. Rev. Lett.*, 1988, vol. 60, p. 1174.
7. Abramyan, P.B., Gulyan, A.M., Kuzanyan, A.S., Petrosyan, A.G., Ter-Mikaelyan, M.L., and Shirinyan, G.O., *JETP Lett.*, 1987, 46 suppl. p. 188.
8. Abramyan, P.B., Gevorgyan, S.G., Kuzanyan, A.S., Melik-Karamova, E.N., Paronyan, T.M., and Terzyan, S.S., *Progress in HTS superconductivity, World Scientific*, 1990, vol. 22, p. 225.
9. Abramyan, P.B., Kuzanyan, A.S., Paronyan, T.M., Terzyan, S.S., and Gulian, A.M., *Progress in HTS superconductivity, World Scientific*, 1990, vol. 22, p. 216.
10. Kuzanyan, A.S. and Paronyan, T.M., *Sov. J. Low Temp. Phys.*, 1991, vol. 17, no. 9, p. 561.
11. Harutunyan, A.R., Grigoryan, L.S., Kuzanyan, A.S., Kuznecov, A.A., Terentiev, A.A., Baron, M., Jasiolek, G., Szymczak, M., and Baszynski, J., *Mod. Phys. Lett. B*, 1991, vol. 5, no. 21, 1447.
12. Kuzanyan, A.S., *J. Contemp. Phys. (Armenian Ac. Sci.)*, 1996, vol. 31, no. 5, p. 20.
13. Jgamadze, V.V., Kokhraidze, R.G., Margiani, N.G., Mestvirishvili, A.N., Odenov, S.V., Papunashvili, N.A., Tsintsadze, G.A., and Shurgaiia, G.A., *Low Temp. Phys.*, 2003, vol. 29, p. 1036.
14. Zhgamadze, V.V., Margiani, N.G., Mzhavanadze, I.A., Sabashvili, N.G., Tsintsadze, G.A., and Shurgaya, G.A., *Low Temp. Phys.*, 2004, vol. 30, p. 937.
15. Margiani, N.G., Nikoghosyan, S.K., Adamia, Z.A., Dzanashvili, D.I., Kuzanyan, V.S., Papunashvili, N.A., Kvartskhava, I.G., Sarkisyan, A.G., and Zhghamadze, V.V., *Int. J. Adv. App. Phy. Res.*, 2016, Special Issue 1, p. 1.
16. Margiani, N.G., Mumladze, G.A., Adamia, Z.A., Kuzanyan, A.S., and Zhghamadze, V.V., *Physica C*, 2018, vol. 548, p. 86.
17. Yau, J.K.F. and Wong, Y.L., *Physica C*, 2000, vol. 339, p. 79.
18. Garnier, V., Monot-Laffez, I., and Desgardin, G., *Physica C*, 2001, vol. 349, p. 103.
19. Abdeen, W., Marahba, S., Awad, R., Abou Aly, A.I., Ibrahim, I.H., and Matar, M., *J. Advanc. Ceram.*, 2016, vol. 5, p. 54.
20. Faalah-Arani, H., Baghshani, S., Sedghi, A., Stornaiuolo, D., Tafuri, F., Massarotti, D., and Riahi-Noori, N., *Ceramics International*, 2018, vol. 44, p. 5209.
21. Oboudi, S.F., *J. Supercond. Nov. Magn.*, 2017, vol. 30, p. 1473.
22. Aftabi, A. and Mozaffari, M., *J. Supercond. Nov. Magn.*, 2015, vol. 28, p. 2337.
23. Cevizci, B., Bilgili, O., and Kosabas, K., *J. Materials Science Materials in Electronics*, 2016, vol. 27, p. 13171.
24. Tepe, M. and Baytosun, F., *J. Supercond. Nov. Magn.*, 2017, vol. 30, p. 3565.
25. Oboudi, S.F. and Mustafa, M.Q., *Advances in Nanoparticles*, 2016, vol. 5, p. 75.
26. Margiani, N.G., Mumladze, G.A., Adamia, Z.A., Papunashvili, N.A., and Dzanashvili, D.I., *J. Supercond. Nov. Magn.*, 2014, vol. 27, p. 397.
27. Polasek, A., Saléh, L.A., Borges, H.A., Hering, E.N., Marinkovic, B., Assunção, F.C.R., Serra, E.T., and Oliveira, G.S., *Mater. Res.*, 2005, vol. 8, p. 391.
28. Duc, T.H., Man, N.K., and Thi, D., *Vietnam Journal of Science and Technology*, 2018, vol. 56, p. 41.

Translated by V. Aroutiounian